Office de la propriété intellectuelle du Canada
Un organisme d'Industrie Canada

Canadian Intellectual Property Office
An Agency of Industry Canada

CA/ 99/01058
24 NOV 1999 (24.11.99)

REC'D 09 DEC 1999
WIPO PCT

CA 99/1058

09/830837

4

Bureau canadien des brevets
Certification

Canadian Patent Office
Certification

La présente atteste que les documents ci-joints, dont la liste figure ci-dessous, sont des copies authentiques des documents déposés au Bureau des brevets.

This is to certify that the documents attached hereto and identified below are true copies of the documents on file in the Patent Office.

Specification and Drawings, as originally filed, with Application for Patent Serial No: **2,,249,648,** on November 4, 1998, by **INSTITUT DE RECHERCHES CLINIQUES DE MONTREAL,** assignee of Nabil G. Seidah, Michel Chrétien and Mieczyslaw Marcinkiewicz, for "Mammalian Subtilisin/Kexin Isozyme Ski-1: A Proprotein Convertase with a Unique Cleavage Specificity".

PRIORITY DOCUMENT
SUBMITTED OR TRANSMITTED IN COMPLIANCE WITH RULE 17.1(a) OR (b)

S. Gregoire
Agent certificateur/Certifying Officer

November 24, 1999
Date

Canada

(CIPO 68)

OPIC CIPO

ABSTRACT OF THE INVENTION

Using RT-PCR and degenerate oligonucleotides derived from the active site residues of subtilisin-kexin-like serine proteinases, we have identified a highly conserved and phylogenetically ancestral human, rat and mouse type-I membrane-bound proteinase called subtilisin-kexin-isozyme-1 (SKI-1). Computer data bank searches reveals that human SKI-1 was previously cloned but with no identified function. *In situ* hybridization demonstrates that SKI-1 mRNA is widely distributed, e.g., in thymus, in adrenal, submaxillary and pituitary glands, in skin, teeth, ribs, intestines, cortex of the kidney and brain, cerebellum, retina, and hippocampus. Cleavage specificity studies show that SKI-1 generates a 28 kDa product from the 32 kDa brain-derived neurotrophic factor precursor (proBDNF) cleaving at an RGLT↓SL bond. In HK293 cells, proSKI-1 processed in two steps at the level of the endoplasmic reticulum and a large fraction of the membrane-bound enzyme is released into the medium. Immunocytochemical analysis shows that SKI-1 is present in the Golgi apparatus and within small punctate structures reminiscent of endosomes. *In vitro* studies suggest that SKI-1 is a Ca^{2+}-dependent serine proteinase exhibiting a wide pH optimum for cleavage of proBDNF.

TITLE OF THE INVENTION:

Mammalian subtilisin/kexin isozyme SKI-1: a proprotein convertase with a unique cleavage specificity.

FIELD OF THE INVENTION:

This invention relates to a serine proteinase capable of converting proteic precursors into mature proteins; particularly a serine proteinase cleaving at non-basic amino acid residues.

BACKGROUND OF THE INVENTION:

Limited proteolysis of inactive precursors to produce active peptides and proteins is an ancient mechanism to generate biologically diverse products from a finite set of genes. Most often, such processing occurs at either single or dibasic residues, as a result of cleavage by a family of mammalian serine proteinases related to bacterial subtilisin and yeast kexin(1, 2). These enzymes, known as pro-protein convertases (PCs), participate in the tissue-specific intracellular processing of precursors at the consensus (R/K)-$(X)_n$-R↓ sequence, where X is any amino acid except Cys and n = 0, 2, 4 or 6 (1-3). PCs have been implicated in the production of various bioactive polypeptide hormones, neuropeptides, enzymes, growth factors, adhesion molecules, cell surface receptors and surface glycoproteins of infectious agents such as viruses and bacteria (1-3).

Less commonly, bioactive products can also be produced by limited proteolysis at amino acids such as Leu, Val, Met, Ala, Thr, Ser and combinations thereof (3). This type of cellular processing has been implicated in the generation of bioactive peptides such as α-and γ-endorphin (4), the C-terminal glycopeptide fragment 1-19 of pro-vasopressin (5), anti-angiogenic polypeptides such as platelet factor 4 (6) and angiostatin (7), the metalloprotease ADAM-10 (8), site 1 cleavage of the sterol receptor element binding proteins (9), as well as in the production of the Alzheimer's amyloidogenic peptides Aβ40, 42 and 43 (10). Processing of this type occurs in the endoplasmic reticulum (ER) (9), or late along the secretory pathway, within secretory

granules (4, 5), at the cell surface, or in endosomes (6-8, 10). So far, the proteinases responsible for thes cleavages have not been unambiguously identified.

Since mammalian convertases process precursors at either single or pairs of basic residues, we hypothesised that a distinct, but related, enzyme(s) may generate polypeptides by cleavage at non-basic residues. To test that idea, we employed an RT-PCR strategy similar to the one used to identify the PCs (11), except that we used degenerate oligonucleotides closer to bacterial subtilisin than to yeast kexin. This approach resulted in the isolation of a cDNA fragment encoding a putative subtilisin-like enzyme from human cell lines. This partial sequence was identical to a segment of a human myeloid cells-derived cDNA reported by Nagase *et al.* (12). A role for this putative subtilase remained undefined up to the present invention.

STATEMENT OF INVENTION:

We show that the sequences of the rat, mouse and human orthologues of this putative type-I membrane-bound subtilisin-kexin-isoenzyme, which we called SKI-1, exhibit a high degree of sequence conservation. Tissue distribution analysis by both Northern blots and *in situ* hybridization (ISH) revealed that SKI-1 mRNA is widely expressed. A stable transfectant of human SKI-1 in HK293 cells allowed the analysis of its biosynthesis and intracellular localization. Finally, we present data demonstrating that SKI-1 cleaves at a specific Thr↓ residue within the N-terminal segment of human pro-brain-derived neurotrophic factor (proBDNF). SKI-1 is the first identified secretory mammalian subtilisin/kexin-like enzyme capable of cleaving a proprotein at non-basic residues.

DESCRIPTION OF THE INVENTION:

This invention will be described hereinbelow by way of specific embodiments and appended figures, which purpose is to illustrate the invention rather than to limit is scope.

BRIEF DESCRIPTION OF FIGURES:

FIG. 1 shows the omparative protein sequences of SKI-1 deduced from rat, mouse and human cDNAs. The position of the predicted end of the 17 aa signal peptide is shown by an arrow. The active sites Asp^{218}, His^{249} and Ser^{414}, as well as the oxyanion hole Asn^{338} are in bold, shaded and underlined characters. The positions of the 6 potential N-glycosylation sites are emphasized in bold. The conserved shaded **CL**DDSHRQK**DC**F**W** sequence fits the consensus signature for growth factors and cytokine receptors family. Each of the two boxed sequences was absent in a number of rat clones. The predicted transmembrane segment is in bold and underlined.

FIG. 2 shows a Northern blot analysis of the expression of SKI-1 in adult rat tissues. **[A]** 5 µg of male rat total RNA were loaded in each lane. Molecular sizes are based on the migration of an RNA ladder. The tissues include: adrenal, thyroid, striatum, hippocampus, hypothalamus, pineal gland, anterior (AP) and neurointermediate (NIL) lobes of the pituitary, submaxillary gland, prostate, ovary and uterus. Notice the high level of SKI-1 mRNA in adrenal glands. **[B]** 2 µg of poly-A+ of (male + female) Sprague Dawley rat adult tissues (Bio/Can Scientific) were loaded, which includes: liver, thymus, spleen, kidney, heart and brain. The estimated size of rat SKI-1 mRNA is about 3.9 kb.

FIG. 3 shows *in situ* hybridization (15 H) of rSKI-1 mRNA in a 2 day old rat. ISH is shown at anatomical resolution on X-ray film using an [^{35}S]-labeled antisense riboprobe **[A-C]** and sense control riboprobe **[D]**. Abbreviations: *Adr* - adrenal gland; *Cb* - cerebellum; *cc* - corpus callosum; *Cx* - cerebral cortex; *H* - heart; *Int* - intestine; *K* - kidney; *Li* - liver; *Lu* - lungs; *M* - muscles; *Mol* - molars; *OT* - olfactory turbinates; *Pit* - pituitary gland; *Rb* - ribs; *Ret* - retina; *Sk* - skin, *SM* - submaxillary gland; *Th* - thymus. Magnification x 4; scale bar (in **D**) = 1cm.

FIG. 4 illustrates the biosynthetic analysis of SKI-1 in HK293 cells. Stable transfectants expressing either the pcDNA3 vector alone or one that expresses SKI-1 (clone 9) were pulse-labeled for 4h with [^{35}S]Met. Media and cell lysates were immunoprecipitated with either a SKI-1 antiserum (Ab: SKI; against aa 634-651) or a pro-SKI-1 antiserum (Pro). The stars represent the 4 specific intracellular proteins (Mr 148, 120, 106 and 98 kDa) immunoprecipitated with the SKI-1 antiserum. In these transfected cells, only the 148 kDa band is recognized by the Pro-antiserum. A 98 kDa immunoreactive SKI-1s protein is also detectable in the medium.

FIG. 5 shows hSKI-1 immunoreactivity in stably transfected HK293 cells. Representation of the comparative double fluorescence staining using a SKI-1 antiserum (directed against aa 634-651) [A] and [B] and FITC-labeled WGA [A'] and [B'] in control [A, A'] and LME-treated [B, B'] cells is shown. Thin arrows emphasize the observed punctate staining which is enhanced in the presence of LME. Large arrows point to the coincident staining of SKI-1 and WGA. Magnification x 900; bar (in B') = 10 µm.

FIG. 6 shows the processing of proBDNF by SKI-1. **[A]** COS-7 cells were infected with vv:BDNF and either vv:WT (-) or vv:SKI-1 in the presence of either vv: PIT or vv:PDX. The cells were metabolically labeled with [^{35}S]Cys-Met for 4h and the media (M) and cell lysates (C) were immunoprecipitated with a BDNF antiserum, prior to SDS-PAGE analysis. The autoradiogram shows the migration positions of proBDNF (32 kDa), the 28 kDa BDNF produced by SKI-1 and the 14 kDa BDNF. **[B]** Microsequence analysis of the [^{35}S]Met-labeled 32 kDa proBDNF (maximal scale 1000 cpm) and [^{3}H]Leu-labeled 28 kDa BDNF (maximal scale 250 cpm), revealing a Met at sequence position 3 and Leu at positions 2, 13 and 14, respectively.

FIG. 7 shows the *in vitro* processing profile of proBDNF by SKI-1. **[A]** pH dependence of the processing of proBDNF by SKI-1. The SKI-1 enzyme preparation was compared to that obtained from the media of Schwann cells infected with the wild type virus (WT) as control. **[B]** Inhibitor profile of the processing of proBDNF to the 28 kDa BDNF by the same SKI-1 preparation as in **[A]**. The reaction was performed overnight at 37°C, pH 6.0. Notice that only PMSF (0.5 mM PMSF+50 µM pAPMSF), o-phenanthroline (5 mM), and EDTA (10 mM) effectively inhibited SKI-1 cleavage of proBDNF.

FIG. 8 shows the *in situ* hybridization translating SKI-1 mRNA expression in the pituitary gland of an adult rat using specific [^{35}S]radiolabeled antisense (*SKI AS*) and control sense (*SKI SS*) riboprobes. The hybridization signal was detected in the anterior (AL), intermediate (IL) and posterior pituitary lobe (PL). Most of the labeling was confined to endocrine cells in AL and IL and to some pituicytes in the PL. Magnification x 5; bar (in b) = 1 mm.

FIG. 9 shows the *in situ* hybridization translating the presence of SKI-1 mRNA sites in the skin of a newborn two days old (p2) rat using antisense (*SKI AS*) and control sense (*SKI SS*) riboprobes. The hybridization signal was detected in the stratum germinativum (small vertical arrows in SGe), in both outer and inner hair sheath (medium arrows) and in some cells within the dermis (D). Other abbreviations: HB - hair bulb, SC - stratum corneum, SGr - stratum granulosum. Magnification x 80.

Fig. 10 shows the *in situ* hybridization (ISH) distribution of SKI-1 mRNA in the rat central nervous system (CNS). ISH distribution pattern in the CNS of adult rat demonstrates a higher concentration of SKI-1 mRNA within a grey matter (GM and all structures indicated with capital letters) vs the white matter (WM) including corpus callosum (cc). Representative brain structures are shown in sagittal (a); horizontal (b) and coronal plane (c - f) after hybridization with antisense SKI-1 riboprobe (a - e) and control sense riboprobe (ssRNA in f). As shown at anatomical level this type of mRNA distribution is highly reminiscent to a type of pan-neuronal gene distribution pattern. As complementary to this figure a Table 1 demonstrates at cellular level the predominance of neuronal SKI-1 mRNA expression over glial SKI-1 mRNA expression. Magnification x 4; bar (in a) = 1 cm. Abbreviations: **CA1** - area 1 of cornus Ammonis; **CA3** - area 3 of cornus Ammonis; **Cb** - cerebellum; **cc** - corpus callosum; **Ch Pl** - choroid plexus; **Cx** - cerebral cortex; **GD** - gyrus dentatus; **GM** - grey matter; **Hip** - hippocamp; **Hy** - hypothalamus; **Ol** - olfactory bulb; **Str** - striatum; **WM** - white matter.

Fig. 11 shows the *in situ* hybridization (ISH) distribution of SKI-1 mRNA in the rat peripheral nervous system (PNS) trigeminal ganglion (TriG). ISH distribution pattern in the CNS of adult rat demonstrates a higher concentration of SKI-1 mRNA within a region of cell bodies (large arrows) over the region of supportive Schwann cells (small arrows). ISH was performed using antisense (SKI-1 as in a) and sense (SKI-1 ss) riboprobes. Magnification x 12.

Fig. 12 shows the distribution of SKI-1, mRNA and/or protein, in the region of spinal cord (SpC) and in the related dorsal root ganglion (DRG) and dorsal root (DR). Demonstrated are the region of neuronal cell bodies in the DRG (SKI-1 mRNA) and the region of nerve terminals in the dorsal horn of the spinal cord (layer I and II) characterized by a especial density of SKI-1 protein.

A) Schematic drawing depicting the position of layer I and II in the dorsal horn as well as that of the related DRG and DR.

B) SKI-1 mRNA revealed by *in situ* hybridization labeling (thin arrows) in the DRG using antisense riboprobes (*SKI-1 AS*).

C) Control hybridization in the DRG using sense riboprobes (*SKI-1 SS*).

D) Immunocytochemical localization of SKI-1 (brown staining) within layer I and II of the dorsal horn and in the dorsal root (DR) suggesting the sensory afferents arriving from DRG. Neuronal and glial nuclei are stained on blue. Magnification x 300.

E) Immunoreactivity of SKI-1 (thin arrows) detected around neuronal somata (large arrows) within layer II of the dorsal horn at high magnification (x 1,500). Pattern of immunoreactive spots is reminiscent to that of axo-somatic or axo-dendritic nerve terminals.

F) Northern blot revealing the concentrations of 4 kb SKI-1 mRNA in different tissues including dorsal root ganglia (DRG) and spinal cord (SpC). Abbreviations: **I** - layer I of the dorsal horn; **II** - layer II of the dorsal horn; **Adr** - adrenal gland; **Cb** - cerebellum; **Cx** - cerebral cortex; **Hip** - hippocamp; **DH** - dorsal horn; **DR** - dorsal root; **DRG** - dorsal root ganglion; **SpC** - spinal cord; **Stom** - stomach and **Thyr** - thyroid gland.

MATERIALS AND METHODS

Polymerase Chain Reaction and Sequencing. Most reverse transcriptase polymerase chain reactions (RT-PCR) were performed using a Titan One Tube RT-PCR system (Boehringer Mannheim) on 1 µg of total RNA isolated from either a human neuronal cell line (IMR-32), mouse corticotrophic cells (AtT20), or rat adrenal glands using a TRIzol reagent kit (Life Technologies). The active site degenerate primers were: <u>His</u> (*sense*) 5'-GGICA(C,T)GGIACI(C,T)(A,T)(C,T)(G,T)(T,G)IGCIGG-3' and <u>Ser</u> (*antisense*) 5'-CCIG(C,T)IACI(T,A)(G,C)IGGI(G,C)(T,A)IGCIACI(G,C)(A,T)GTICC-3' based on the sequences GHGT(H,F)(V,C)AG and GTS(V,M)A(T,S)P(H,V)V(A,T)G, respectively. The amplified 525 bp products were sequenced on an ALF DNA sequencer (Pharmacia). To obtain the full length of rat and mouse SKI-1, we used PCR primers based on the human (12) and mouse sequences, in addition to 5' (13) and 3' (14) RACE amplifications. To avoid errors, at least three clones of the amplified cDNAs were fully sequenced. The GenBank accession numbers of the 3788 bp mouse mSKI-1 cDNA and 3895 bp rat rSKI-1 are AF094820 and AF094821, respectively.

Transf ction and Metab lic Labeling. Human SKI-1 (nt 1-4338) (12) in Bluescript (a generous gift from Dr. N. Nomura, Kazusa DNA Research Institute, Chiba, Japan; gene name KIAA0091, accession No. D42053) was digested with SacII (nt 122-4338) and inserted into the vector PMJ602. The construct was digested with 5' KpnI/3' NheI, cloned into the KpnI/XbaI sites of pcDNA3 (Invitrogen), and the cDNA transfected into HK293 cells with a DOSPER liposomal transfection reagent (Boehringer Mannheim). A number of stable transfectants resistant to G418 and positive on western blots using a SKI-1 antiserum (*see below*) were isolated, and one of them (clone 9), was further investigated. Cells were pulsed for 4h with [^{35}S]Met and the media and cell lysates immunoprecipitated with SKI-1 antisera directed against either amino acids (aa) 634-651, or aa 217-233, or a pro-SKI-1 antiserum directed against the pro-segment comprising aa 18-188 (Fig. 1). Immune complexes were resolved by SDS-PAGE on a 6% polyacrylamide/Tricine gel (15).

Northern Blots, *in situ* Hybridizations and Immunocytochemistry. Northern blot analyses (16) were done on total RNA from adult male rat tissues using either a TRIzol reagent kit (Life Technologies) or a Quick Prep RNA-kit (Pharmacia)and on polyA+ RNA of (male + female) rat adult tissues (Bio/Can Scientific). The blots were hybridized overnight at 68°C in the presence of [^{32}P]UTP SKI-1 cRNA probes, consisting of the antisense of nucleotides 655-1249 of rat SKI-1 (accession No. AF094821). For ISH, the same rat sense and antisense cRNA probes were doubly labeled with uridine and cytosine 5'-{λ-[^{35}S]thio}triphosphate (16). The distribution of SKI-1 mRNA in different tissues of adult and newborn rat (P1) after emulsion autoradiography was investigated. Relative densities of specific SKI-1 mRNA labeling per cell in selected organs have been measured upon counting of silver grains produced by antisense SKI-1 riboprobes and subtraction of non-specific background produced with sense SKI-1 riboprobes. Countings were made under 1000-fold microscopical magnification in the similar regions of adjacent sections stained with hematoxylin and eosin. Results are the mean (S.E.D. of 10 - 16 readings / cell type. Newborn rats were frozen at - 35°C in isopentane and then cut into 14-µm sagital cryostat sections (1, 16). After hybridization, all tissue slides were exposed for 4 or 30 days to X-Ray film or emulsion autoradiography, respectively. For immunofluorescence staining we used a rabbit anti-SKI-1 antiserum at a 1:100 dilution and rhodamine-labeled goat anti-rabbit IgGs diluted 1:20 (16). Red SKI-1 immunostaining was compared with green staining patterns of both fluorescein-labeled concavalin A (ConA;

Molecular Probes, OR), an ER marker, or fluorescein-conjugated wheat germ agglutinin (WGA; Molecular Probes, OR), a Golgi marker (17).

***Ex vivo* and *in vitro* proBDNF Processing.** A vaccinia virus recombinant of human SKI-1 (vv:SKI-1) was isolated as previously described for human proBDNF (vv:BDNF) (15). The vaccinia virus recombinants of the serpins α1-antitrypsin Pittsburgh (α1-PIT; vv:PIT) and α1-antitrypsin Portland (α1-PDX; vv:PDX) (18) were generous gifts from Dr. G. Thomas (Vollum Institute, Portland, OR). For analysis of the cleavage specificity of hSKI-1, 4 x10^6 COS-7 cells were co-infected with 1 pfu/cell of vv:BDNF and either the wild type virus (vv:WT) alone at 2 pfu/cell or with 1 pfu/cell of each virus in the combinations: [vv:SKI-1+vv:WT], [vv:SKI-1+vv:PIT] and [vv:SKI-1+vv:PDX]. At 10h post infection, cells were pulse labeled for 4h with 0.2 mCi [^{35}S]Cys-Met (Dupont). Media and cell extracts were immunoprecipitated with a BDNF antiserum (19; kindly provided by Amgen) at a concentration of 0.5 µg/ml. The precipitates were resolved on polyacrylamide gradient gels (13-22%) and the autoradiograms obtained as described (15). Microsequencing analysis was performed on the [^{35}S]Met-labeled 32 kDa proBDNF and [^{3}H]Leu-labeled 28 kDa BDNF, as described (20). For *in vitro* analysis, the 32 kDa proBDNF obtained from the media of LoVo cells infected with vv:BDNF was incubated overnight with the shed form of SKI-1 obtained from rat Schwann cells (16) co-infected with vv:SKI-1 and vv:PDX, either at different pHs or at pH 6.0 in the presence of selected inhibitors: pepstatin (1 µM), antipain (50 µM), cystatin (5 µM), E64 (5 µM), soya bean trypsin inhibitor (SBTI, 5 µM), 0.5 M phenylmethylsulfonyl fluoride (PMSF) + 50 µM para-aminophenylmethylsulfonyl fluoride (pAPMSF), o-phenanthroline (5 mM) and EDTA (10 mM). The products were resolved by SDS-PAGE on a 15% polyacrylamide gel, transferred to a PVDF membrane and then probed with a BDNF antiserum (Santa Cruz) at a dilution of 1:1000.

RESULTS

Protein Sequence Analysis of SKI-1. We first aligned the protein sequences within the catalytic domain of PC7 (21), yeast subtilases and bacterial subtilisins, together with that of a novel subtilisin-like enzyme from *Plasmodium falciparum* (J-C. Barale *et al., submitted*). This led to the following choice of conserved amino acids around the active sites His and Ser: GHGT(H/F)(V/C)AG and GTS(M/V)A(T/S)P(H/V)V(A/T)G, respectively. Thus, using degenerate oligonucleotides

coding for the sense His and antisense Ser consensus sequences we initiated a series of RT-PCR reactions on total RNA (*see Materials and Methods*) and isolated a 525 bp cDNA fragment from the human neuronal cell line IMR-32. This sequence was found to be 100% identical to that reported for a human cDNA called KIAA0091 (Accession No. D42053) obtained from a myeloid KG-1 cell line (12) and 88 % identical to that of a 324 bp EST sequence (Accession No. H31838) from rat PC12 cells. We next completed the rat and mouse cDNA sequences following RT-PCR amplifications of total RNA isolated from rat adrenal glands and PC12 cells, and from mouse AtT20 cells. Starting from the equivalent rat and mouse 525 bp fragments, the complete sequences were determined using a series of RT-PCR reactions with human-based oligonucleotides in addition to 5' (13) and 3' (14) RACE protocols. As shown in Fig. 1, alignment of the protein sequence deduced from the cDNAs of rat, mouse and human SKI-1 revealed a high degree of conservation. Rat and mouse SKI-1 share 98% sequence identity and a 96% identity to human SKI-1. Interestingly, within the catalytic domain (Asp^{218} to Ser^{414}) the sequence similarity between the three species is 100%. Analysis of the predicted amino acid sequence suggests a 17 aa signal peptide, followed by a putative pro-segment beginning at Lys^{18} and extending for some 160-180 amino acids. The proposed catalytic domain encompasses the typical active sites Asp^{218}, His^{249} and Ser^{414} and the oxyanion hole Asn^{338}. This domain is followed by an extended C-terminal sequence characterized by the presence of a conserved growth factor / cytokine receptor family motif $\underline{C}^{849}\underline{L}DDSHRQK\underline{DC}F\underline{W}^{861}$. This sequence is then followed by a potential 24 aa hydrophobic transmembrane segment and a less conserved 31 aa cytosolic tail that remarkably consists of 35% basic residues. Some of the clones isolated from rat adrenal glands suggested the existence of alternatively spliced rSKI-1 mRNAs in which the segments coding for aa 430-483 or 858-901 are absent. Finally, the phylogenetic tree derived from the alignment of the catalytic domain of SKI-1 with subtilases (22) suggests that it is an ancestral protein that is closer to plant and bacterial subtilases than to either yeast or mammalian homologues (*not shown*).

Tissue Distribution of SKI-1 mRNA. Northern blot analyses of SKI-1 mRNA in adult male rat tissues reveal that rSKI-1 mRNA is widely expressed and is particularly rich in anterior pituitary, thyroid and adrenal glands (Figs. 2A and 8). A Northern blot of polyA+ RNA obtained from mixed adult male and female rat tissues also showed a wide distribution and a particular enrichment in liver (Fig. 2B). Similarly, analysis of 24 different cell lines (23) revealed a ubiquitous expression of SKI-1 mRNA (*not shown*).

In situ hybridization data obtained in a day 2 postnatal rat also provided evidence of a widespread, if not ubiquitous distribution of rSKI-1 mRNA. Figure 3 shows at the anatomical level the presence of SKI-1 mRNA in developing skin (see also Figure 9), striated muscles, cardiac muscles, bones and teeth as well as brain and many internal organs. Strong hybridization signals were detectable in the retina, cerebellum, pituitary, submaxillary, thyroid and adrenal glands, molars, thymus, kidney and intestine. Evidence for the cellular expression of rSKI-1 mRNA was obtained from analysis of the relative labeling densities per cell in selected tissues, based on a semiquantitative analysis of emulsion autoradiographies (*not shown*). In the central nervous system (CNS) rSKI-1 mRNA labeling was mostly confined to neurons, whereas ependymal cells, supportive glial cells, such as presumed astrocytes, oligodendrocytes, and microglia, exhibited 5-30 fold less labeling/cell (see Table 1 and Figure 10). In addition, within the peripheral nervous system (PNS) trigeminal ganglia reveal a 5-10 fold greater expression in neurons as compared to presumptive Schwann cells (Figures 11 and 12 and Table 1). Labeling was observed in most of the glandular cells in the anterior and intermediate lobes of the pituitary as well as in the pituicytes of the pars nervosa. A semiquantitative comparison in the adult and newborn rat pituitary gland, submaxillary gland, thymus and kidney demonstrated an overall 2-fold decreased labeling of rSKI-1 mRNA with age (*not shown*).

Biosynthesis of hSKI-1. To define the molecular forms of human SKI-1 and their biosynthesis, we generated both a vaccinia virus recombinant (vv:SKI-1) and a stable transfectant in HK293 cells. Three antisera were produced against aa 18-188 (prosegment), 217-233 and 634-651 of SKI-1. Expression of vv:SKI-1 in 4 different cell lines revealed that the enzyme is synthesized as a 148 kDa proSKI-1a zymogen which is processed into 120, 106 and 98 kDa proteins. In this system, both the 148 and 120 kDa forms are recognized by the Pro-domain antiserum, whereas all 4 forms react with the other two antisera. Processing of the 148 kDa proSKI-1a into the 120 and 106 kDa

forms occurs in the ER based on the presence of these proteins in cells pre-incubated with the fungal metabolite brefeldin A (see 24 for refs., *not shown*). The same SKI-1-related forms are also observed in stably transfected HK293 cells following a 4h pulse labeling with [^{35}S]Met (Fig.4). The results reveal the intracellular formation of a secretable 98 kDa form (SKI-1s) recognized by both of the SKI antisera but not by the Pro antiserum. These data demonstrate that the 148 kDa proSKI-1a is N-terminally cleaved into an intermediate 120 kDa form containing part of the prosegment (proSKI-1b) which is then further excised to form a non secretable 106 kDa SKI-1. This suggests that two cleavages occur within the prosegment prior to the formation of the presumably membrane-bound 106 kDa form which is later shed into the medium as a 98 kDa soluble SKI-1s.

Intracellular localization of SKI-1. Double staining immunofluorescence was used to compare the intracellular localization of the stably transfected human SKI-1 in HK293 cells and that of either the ER or Golgi markers ConA and WGA (17), respectively. The data show that SKI-1 exhibits: **(i)** peripheral nuclear staining, colocalizing with ConA fluorescence, presumably corresponding to the ER (*not shown*); **(ii)** paranuclear staining colocalizing with WGA fluorescence, suggesting the presence of SKI-1 in the Golgi (Fig. 5A,B) and **(III)** punctate staining observed in the cytoplasm and within extensions of a few cells (Fig. 5A). Some, but not all of the punctate immunostaining matched that observed with WGA. This suggests that SKI-1 localizes in the Golgi but may sort to other organelles, including lysosomal and/or endosomal compartments. Since in HK293 cells we observed scant immunoreaction to either cathepsin B or cathepsin D (*not shown*), we could not directly assess the presence of SKI-1 within lysosomes. An indication of lysosomal/endosomal localization was provided by the analysis of SKI-1 immunofluorescence within cells pre-incubated for 4h with 10 mM leucine-methyl ester (LME), a specific lysosomal/endosomal protease inhibitor (25). The results showed a net increase in the proportion of cells exhibiting punctate staining (Fig. 5C) as compared to control cells. Thus, SKI-1 immunoreactivity is enhanced upon LME inhibition of lysosomal/endosomal hydrolases.

Enzymatic Activity and Cleavage Specificity of SKI-1. To prove that SKI-1 is a proteolytic enzyme we examined its ability to cleave five different potential precursor substrates. Our choice was based on the tissue expression pattern of SKI-1 (Figs. 2, 3), which led us to select pro-opiomelanocortin (pituitary), pro-atrial natriuretic factor (heart), HIV gp160 (T-lymphocytes) and based on its neuronal expression, pro-nerve growth factor and pro-brain-derived neurotrophic factor (proBDNF). Cellular co-expression of vv:SKI-1 with the vaccinia virus recombinants of each of the above precursors revealed that only proBDNF could be cleaved intracellularly by SKI-1. Thus, upon expression of vv:BDNF alone in COS-7 cells we observed a partial processing of proBDNF (32 kDa) into the known major 14 kDa BDNF product (15), and the minor production of a previously observed (16; Mowla, S.J. *et al., submitted*) but still undefined 28 kDa product (Fig. 6A). Upon co-expression of proBDNF and SKI-1, a net increase in the level of the secreted 28 kDa BDNF is evident, without significant alteration in the amount of 14 kDa BDNF (Fig. 6A). To examine whether the 28 kDa product results from cleavage at a basic residue or at an alternative site, we first co-expressed proBDNF, SKI-1 and either α1-PIT or α1-PDX which are inhibitors of thrombin and PC cleavages, respectively (18, 26). The results show that different from α1-PIT, the serpin α1-PDX selectively blocks the production of the 14 kDa BDNF and that neither α1-PIT nor α1-PDX affect the level of the 28 kDa product. This demonstrates that α1-PDX effectively inhibits the endogenous furin-like enzyme(s) responsible for the production of the 14 kDa BDNF (15), but does not inhibit the ability of SKI-1 to generate the 28 kDa product. Thus, it is likely that the generation of the 28 kDa BDNF takes place via an alternate cleavage. Incubation of the cells with the Ca^{2+} ionophore A23187 abolished the production of both the 14 and 28 kDa products (*not shown*), supporting the notion that similar to the PCs (1-3, 24), SKI-1 is a Ca^{2+}-dependent enzyme.

In Fig. 6B, we present the N-terminal microsequence analysis of [^{35}S]Met-labeled 32 kDa proBDNF and [^{3}H]Leu-labeled 28 kDa BDNF. The sequence of the 32 kDa form revealed the presence of an [^{35}S]Met at position 3 (Fig. 6B), which is in agreement with the proposed sequence of human proBDNF (27) resulting from the removal of an 18 aa signal peptide cleaved at GCMLA^{18}↓APMK site. The N-terminal sequence of the 28 kDa product revealed a [^{3}H]Leu at positions 2, 13 and 14 (Fig. 6B). This result demonstrates the 28 kDa BDNF is generated by a unique cleavage at Thr^{57} in the sequence: RGLT^{57}↓SLADTFEHVIEELL (27).

To prove that SKI-1 is directly responsible for the production of the 28 kDa BDNF at the novel Thr-directed cleavage, we performed *in vitro* studies. Thus, proBDNF was incubated at various pHs with concentrated media of vv:SKI-1-infected Schwann cells. A similar preparation obtained from wild type vaccinia virus-infected cells served as control. The data show that SKI-1 exhibits a wide pH dependence profile revealing activity at both acidic and neutral pHs between pH 5.5 up to 7.3 (Fig. 7A) but also at pH 4.5 and 8 (*not shown*). Analysis of the inhibitory profile of this reaction revealed that metal chelators such as EDTA and o-phenanthroline, or a mixture of the serine proteinase inhibitors PMSF + pAPMSF effectively inhibit the processing of proBDNF by SKI-1. The inhibition by EDTA is expected since like all PCs, SKI-1 is a Ca^{2+}-dependent enzyme. The unexpected inhibition by 5 mM o-phenanthroline may be due to excess reagent since at 1 mM only 25% inhibition is observed (*not shown*). All other class-specific proteinase inhibitors (aspartyl-, cysteinyl-, and serine proteases- of the trypsin-type) proved to be inactive.

Table 1

Tissue	Adult Silver grains/Cell ± SED	Newborn (PI) Silver Grains/Cell ±SED
C.N.S.		
Cerebal Cortex		
Neurons, large	19.7 ± 5.8	ND*
Neurons, medium & small	5.7 ± 2.3	
Astrocytes, presumptive	0.6 ± 0.5	
Hippocampus		ND
Neurons, pyramidal	15.3± 3.9	
Neurons, granules	23.7 ± 5.3	
Corpus callosum		ND
Oligodendrocytes, presumpt.	0.6 ± 0.6	
Spinal cord		ND
Motorneurons	27.8 ± 7.1	
Circumventricular organs		ND
Plexus choroideux	9.6 ± 1.9	
Ependyma (III ventr.)	2.9 ± 0.8	

P.N.S.		ND
Trigeminal ganglion		
Neurons, large	14.6 ± 4	
Satellite cells	3.8 ± 22	
Schwann cells, presumpt.	1.3 ± 1.9	
Pituitary gland		
Anterior lobe cells	4.9 ± 3.6	9.3 ± 2.1
Intermediate lobe cells	4.1 ± 0.9	7.2 ± 1.4
Posterior lobe pituicytes	3.6 ± 3.9	6.7 ± 4.2
Thymus		
Cortical lymphocytes	4.1 ± 0.7	7.1 ± 1.0
Medullary reticular cells	2.7 ± 1.0	4.4 ± 0.9
Adipocytes	0.3 ± 0.6	ND
Fibroblats	0.2 ± 0.1	ND
Submaxillary gland		
Epithelial cells	2.1 ± 1.0	3.9 ± 1.7
Acinar cells	2.4 ± 1.2	4.5 ± 1.7
Kidney		
Glomerular cells	2.8 ± 0.9	4.2 ± 0.9
Convoluted tubules	4.1 ± 2.7	9.8 ± 1.4

*ND = not determined

DISCUSSION

This work provides the first evidence for the existence of a mammalian secretory Ca^{2+}-dependent serine proteinase of the subtilisin-kexin type that selectively cleaves at non-basic residues. Thus, SKI-1 processes the 32 kDa human proBDNF at an **K**AGS**R**GL**T**↓SL sequence generating a 28 kDa form, which may have its own biological activity (Mowla, S.J. *et al., submitted*). Such a cleavage site is close to the consensus site deduced from a large body of work done with the PCs, whereby an **(R/K)**-$(X)_n$-**R**↓X-**(L/I/V)**, [where n=0, 2, 4 or 6] motif is favored by most PCs (1-3, 28). Note that in the SKI-1 site, P1 Arg is replaced by Thr and an aliphatic Leu is present

at P2', an amino acid also favored by PCs (1-3, 28). Several proteins are known to be cleaved following Thr. These include human anti-angiogenic platelet factor 4 (6; QCLCVKTT↓SQ) and angiostatin (7; KGPWCFTT↓DP), the neuroendocrine α-endorphin (4; KSQTPLVT↓LF), the ADAM-10 metalloprotease (8; LLRKKRTT↓SA), as well as the amyloidogenic peptide Aβ43 (10; VGGVVIAT↓VI).

Interestingly, comparison of the phylogenetically highly conserved sequence of proBDNF revealed an insertion of hydroxylated amino acids (Thr and Ser) just after the identified SKI-1 cleavage site of human proBDNF. Thus, in rat and mouse proBDNF, two threonines are inserted (RGLTTT—SL) and in porcine proBDNF five serines added (RGLTSSSSS—SL) (27). These observations raise a number of questions: (i) do these insertions affect the kinetics of proBDNF cleavage by SKI-1? (ii) does SKI-1 recognize both single and pairs of Thr and Ser and combinations thereof? (iii) is the presence of a basic residue at P4, P6 or P8 important for cleavage? and (iv) similar to enzymes cleaving at basic residues (29), does the possible phosphorylation at specific Thr or Ser residues affect substrate cleavability by SKI-1?

Biosynthetic analysis of the zymogen processing of proSKI-1 demonstrated a two-step ER-associated removal of the pro-segment (Fig. 4). Furthermore, analysis of the [$^{35}SO_4$]-labeled SKI-1 demonstrated only the presence of sulfated 106 and 98 kDa forms but not that of either the 148 or 120 kDa forms recognized by the Pro-segment antiserum (*not shown*). Since sulfation occurs in the *trans* Golgi network, this confirms that the removal of the pro-segment occurs in the ER. Like furin and PC5-B (1-3, 24) the membrane bound 106 kDa SKI-1 is transformed into a soluble 98 kDa form that is released into the medium by an as yet unknown mechanism. The secreted 98 kDa SKI-1s is enzymatically active since it processes proBDNF *in vitro* (Fig. 7). Numerous attempts to sequence the SDS-PAGE purified [^{3}H]Leu and Val-labeled 148 kDa and 98 kDa forms, resulted in ambiguous results, suggesting that SKI-1 is refractory to N-terminal Edman degradation. Presently, we cannot define the two zymogen cleavage sites leading to the sequential formation of the 120 kDa proSKI-1b and 106 kDa SKI-1 deduced by pulse (Fig. 4) and pulse-chase studies (*not shown*). Examination of the pro-segment sequence (Fig. 1), the species-specific proBDNF motif potentially recognized by SKI-1 (*see above*), and the alignment of SKI-1 with other subtilases (22), suggests two possible conserved sites: RNNPSS^{95}↓DYPS and RHSS^{182}↓RRLL. Both sites predict a cleavage after pairs of Ser with either a P6 or a P4 Arg, respectively.

Phylogenetic structural analysis of the predicted amino acid sequence of SKI-1 reveals that this serine proteinase is closer to plant and bacterial subtilases than it is to yeast and mammalian PCs. The 100% conservation of the catalytic domain sequence, although striking and suggestive of an important function, is not far from the 98% similarity between human and rat PC7 (3, 21). The sequence C-terminal to the catalytic domain of SKI-1 is very different from that of any of the known PCs. In fact, although PCs have a typical P-domain critical for the folding of these enzymes (for reviews see 1-3), we did not find the hallmark sequences (3, 30) of the P-domain within the SKI-1 structure. Instead different from the PCs, we find a conserved growth factor/cytokine receptor motif of which functional importance will need to be addressed, especially since this motif is partly missing in alternatively spliced forms (Fig. 1). Finally, the highly basic nature of the cytosolic tail of SKI-1 (Fig. 1) may be critical for its probable cellular localization within endosomal/lysosomal compartments (Fig. 5), similar to the importance of basic residues for the accumulation of the α-amidation enzyme PAM in endosomal compartments (Milgram, S.L., *personal communication*).

The wide tissue distribution of SKI-1 mRNA transcripts suggests that this enzyme processes numerous precursors in various tissues. Furthermore, the observed developmental down-regulation of the level of its transcripts also suggests a functional importance during embryonic development. The fact that SKI-1 can cleave C-terminal to Thr and possibly Ser residues suggests that, like the combination of PCs and carboxypeptidases E and D (31), a specific carboxypeptidase may also be required to trim out the newly exposed C-terminal hydroxylated residues. Such a hypothesis may find credence in a report suggesting that the amyloidogenic Aβ43 (ending at Thr) may be transformed *in vitro* into Aβ42 and Aβ40 by a brain-specific carboxypeptidase(s) (32).

A recent report demonstrated the existence of a soluble subtilisin-like enzyme exhibiting a 29% sequence identity to SKI-1 in *Plasmodium falciparum* merozoites (PfSUB-1). This enzyme localizes to granular-like compartments and presumably cleaves at a Leu↓Asn bond (33). In that context, SKI-1 may represent the first member of an as yet undiscovered mammalian family of proteinases implicated in the limited proteolysis of proproteins at sites other than basic amino acids that may differ by their intracellular localization and cleavage specificity.

This invention has been described in details hereinabove, and it will be readily apparent to the skilled artisan that modifications can be made thereto without departing

form the teachings of the present disclosure. These modifications are considered within th scope of the present invention, as defined in th appended claims.

REFERENCES

1. Seidah, N.G., Day, R., Marcinkiewicz, M., & Chrétien, M. (1998) *Ann. N.Y. Acad. Sci.* **839**, 9-24.
2. Steiner, D.F. (1998) *Curr. Opin. Chem. Biol.* **2**, 31-39.
3. Seidah, N.G., Mbikay, M., Marcinkiewicz, M., & Chrétien, M. (1998) in *Proteolytic and Cellular Mechanisms in Prohormone and Neuropeptide Precursor Processing*, ed. Hook, V.Y.H. (R.G. Landes Company, Georgetown, TX), pp. 49-76.
4. Ling, N., Burgus, R., & Guillemin, R. (1976) *Proc. Natl. Acad. Sci. USA* **73**, 3042-3046.
5. Burbach, J.P.H., Seidah, N.G., & Chrétien, M. (1986) *Eur. J. Biochem.* **156**, 137-142.
6. Gupta, S.K., Hassel, T., & Singh, J.P. (1995) *Proc. Natl. Acad. Sci. USA* **92**, 7799-7803.
7. O'Reilly, M.S., Holmgren, L., Shing, Y., Chen, C., Rosenthal, R.A., Moses, M., Lane, W.S., Cao, Y., Sage, E.H., & Folkman, J. (1994) *Cell* **79**, 315-328.
8. Rosendahl, M.S., Christine Ko, S., Long, D.L., Brewer, M.T., Rosenzweig, B., Hedl, E., Anderson, L., Pyle, S.M., Moreland, J.,Meyers, M.A., Kohno, T., Lyons, D., & Lichenstein, H.S. (1997) *J. Biol. Chem.* **272**, 24588-24593.
9. Duncan, E.A., Brown, M.S., Goldstein, J.L., & Sakai, J. (1997) *J. Biol. Chem.* **272**, 12778-12785.
10. Checler, F. (1995) *J. Neurochem.* **65**, 1431-1444.
11. Seidah, N.G. (1995) *Methods Neurosci.* **23**, 3-15.
12. Nagase, T., Miyajima, N., Tanaka, A., Sazuka, T., Seki, N., Sato, S., Tabata, S., Ishikawa, K-I., Kawarabayasi, Y., Kotani, H., & Nomura, N. (1995) *DNA Res.* **2**, 37-43.
13. Edwards, J.B.D.M., Delort, J., & Mallet, J. (1991) *Nucl. Acid. Res.* **19**, 5227-5232.
14. Lusson, J., Vieau, D., Hamelin, J., Day, R., Chrétien, M., & Seidah, N.G. (1993) *Proc Natl Acad Sci USA* **90**, 6691-6695.

15. Seidah, N.G., Benjannet, S., Pareek, S., Chrétien, M., & Murphy, R.A. (1996) *FEBS Lett.* **379**, 247-250.

16. Marcinkiewicz, M., Savaria, D., & Marcinkiewicz, J. (1998) *Mol. Brain Res.* **59**, 229-246.

17. Lippincott-Schwartz, J., Youan, L.C., Bonifacino, J.S., & Klausner, R.D. (1989) *Cell* **56**, 801-813.

18. Anderson, E.D., Thomas, L., Hayflick, J.S., & Thomas, G. (1993) *J. Biol. Chem.* **268**, 24887-24891.

19. Yan, Q., Rosenfeld, R.D., Matheson, C.R., Hawkins, N., Lopez, O.T., Bennett, L., & Welcher, A.A. (1997) *Neuroscience* **78**, 431-448.

20. Paquet, L., Bergeron, F., Seidah, N.G., Chrétien, M., Mbikay, M., & Lazure, C. (1994) *J. Biol. Chem.* **269**, 19279-19285.

21. Seidah, N.G., Hamelin, J., Mamarbachi, M., Dong, W., Tadros, H., Mbikay, M., Chrétien, M., & Day, R. (1996) *Proc. Natl. Acad. Sci. USA* **93**, 3388-3393.

22. Siezen, R.J., & Leunissen, J.A.M. (1997) *Protein Sci.* **6**, 501-523.

23. Seidah, N.G., Day, R., & Chrétien, M. (1994) *Biochimie* **76**, 197-209.

24. de Bie, I., Marcinkiewicz, M., Malide, D., Lazure, C., Nakayama, K., Bendayan, M., & Seidah, N.G. (1996) *J. Cell Biol.* **135**, 1261-1275.

25. Reeves, J.P., Decker, R.S., Crie, J.S., & Wildenthal, K. (1981) *Proc. Natl. Acad. Sci. USA* **78**, 4426-4429.

26. Benjannet, S., Savaria, D., Laslop, A., Chrétien, M., Marcinkiewicz, M., & Seidah, N.G. (1997) *J. Biol. Chem.* **272**, 26210-26218.

27. Maisonpierre, P.C., Le Beau, M.M., Espinosa, R., Ip, N.Y., Belluscio, L., de la Monte, S.M., Squinto, S., Furth, M.E. & Yancoupolos, G.D. (1991) *Genomics* **10**, 558-568.

What is claimed is:

1. A method for cleaving a proteic precursor recognizable and cleavable at the C-terminal end of a threonine or a serine residue, which comprises the step of contacting said proteic precursor with and enzyme having an amino acid sequence as shown in Figure 1, a variant thereof or an enzymatically active part thereof.

2. A method as defined in claim 1, wherein said proteic precursor is a 32 kDa brain-derived neutrotrophic factor precursor (proBDNF).

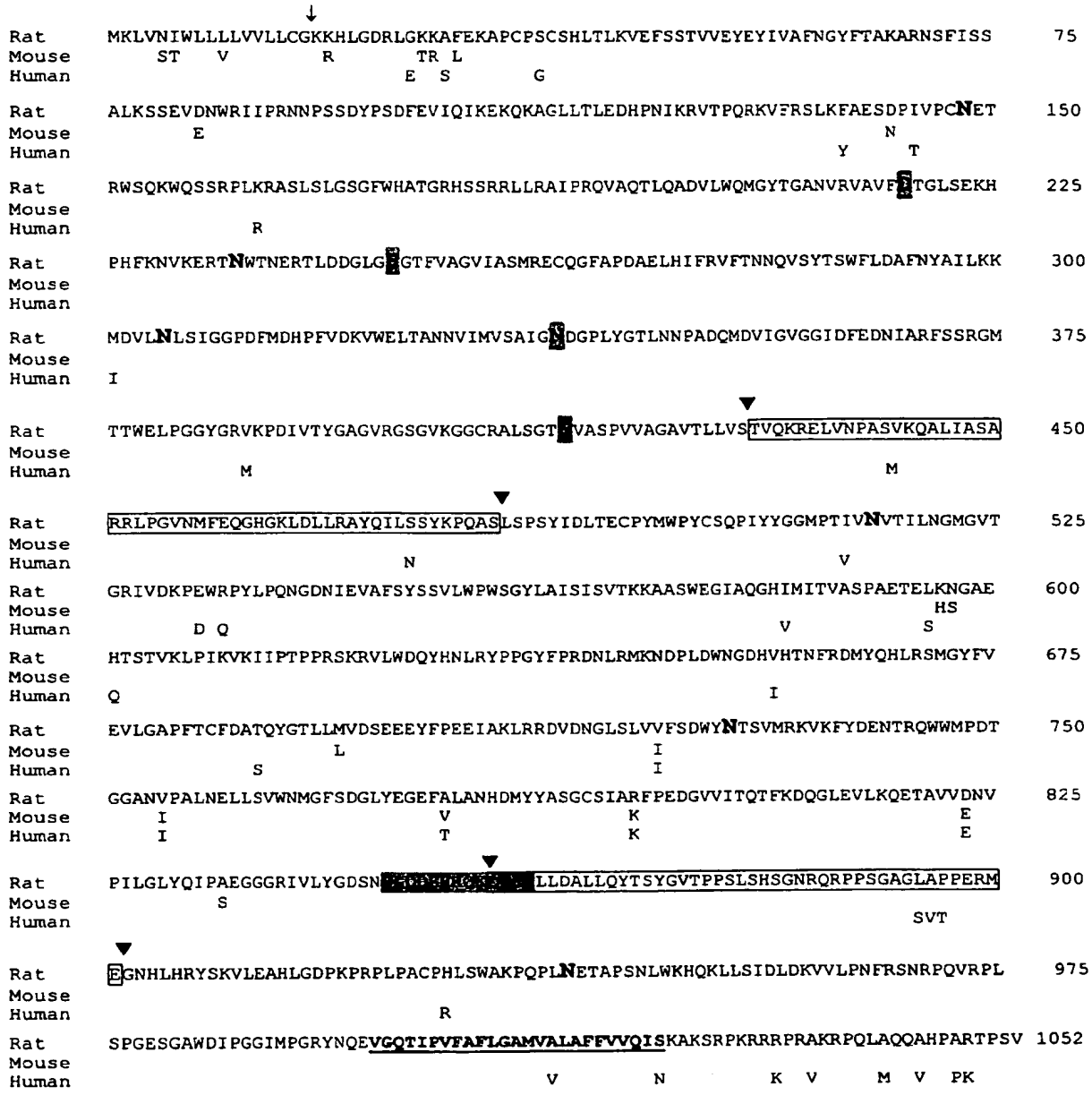
Rat MKLVNIWLLLLVVLLCGKKHLGDRLGKKAFEKAPCPSCSHLTLKVEFSSTVVEYEYIVAFNGYFTAKARNSFISS 75
Mouse ST V R TR L
Human E S G
Rat ALKSSEVDNWRIIPRNNPSSDYPSDFEVIQIKEKQKAGLLTLEDHPNIKRVTPQRKVFRSLKFAESDPIVPCNET 150
Mouse E N
Human Y T
Rat RWSQKWQSSRPLKRASLSLGSGFWHATGRHSSRRLLRAIPRQVAQTLQADVLWQMGYTGANVRVAVFETGLSEKH 225
Mouse
Human R
Rat PHFKNVKERTNWTNERTLDDGLGIGTFVAGVIASMRECQGFAPDAELHIFRVFTNNQVSYTSWFLDAFNYAILKK 300
Mouse
Human
Rat MDVLNLSIGGPDFMDHPFVDKVWELTANNVIMVSAIGNDGPLYGTLNNPADQMDVIGVGGIDFEDNIARFSSRGM 375
Mouse
Human I
Rat TTWELPGGYGRVKPDIVTYGAGVRGSGVKGGCRALSGTSVASPVVAGAVTLLVSTVQKRELVNPASVKQALIASA 450
Mouse
Human M M
Rat RRLPGVNMFEQGHGKLDLLRAYQILSSYKPQASLSPSYIDLTECPYMWPYCSQPIYYGGMPTIVNVTILNGMGVT 525
Mouse
Human N V
Rat GRIVDKPEWRPYLPQNGDNIEVAFSYSSVLWPWSGYLAISISVTKKAASWEGIAQGHIMITVASPAETELKNGAE 600
Mouse HS
Human D Q V S
Rat HTSTVKLPIKVKIIPTPPRSKRVLWDQYHNLRYPPGYFPRDNLRMKNDPLDWNGDHVHTNFRDMYQHLRSMGYFV 675
Mouse
Human Q I
Rat EVLGAPFTCFDATQYGTLLMVDSEEEYFPEEIAKLRRDVDNGLSLVVFSDWYNTSVMRKVKFYDENTRQWWMPDT 750
Mouse L I
Human S I
Rat GGANVPALNELLSVWNMGFSDGLYEGEFALANHDMYYASGCSIARFPEDGVVITQTFKDQGLEVLKQETAVVDNV 825
Mouse I V K E
Human I T K E
Rat PILGLYQIPAEGGGRIVLYGDSNLLDALLQYTSYGVTPPSLSHSGNRQRPPSGAGLAPPERM 900
Mouse S
Human SVT
Rat EGNHLHRYSKVLEAHLGDPKPRPLPACPHLSWAKPQPLNETAPSNLWKHQKLLSIDLDKVVLPNFRSNRPQVRPL 975
Mouse
Human R
Rat SPGESGAWDIPGGIMPGRYNQEVGQTIPVFAFLGAMVALAFFVVQISKAKSRPKRRRPRAKRPQLAQQAHPARTPSV 1052
Mouse
Human V N K V M V PK

FIGURE 1

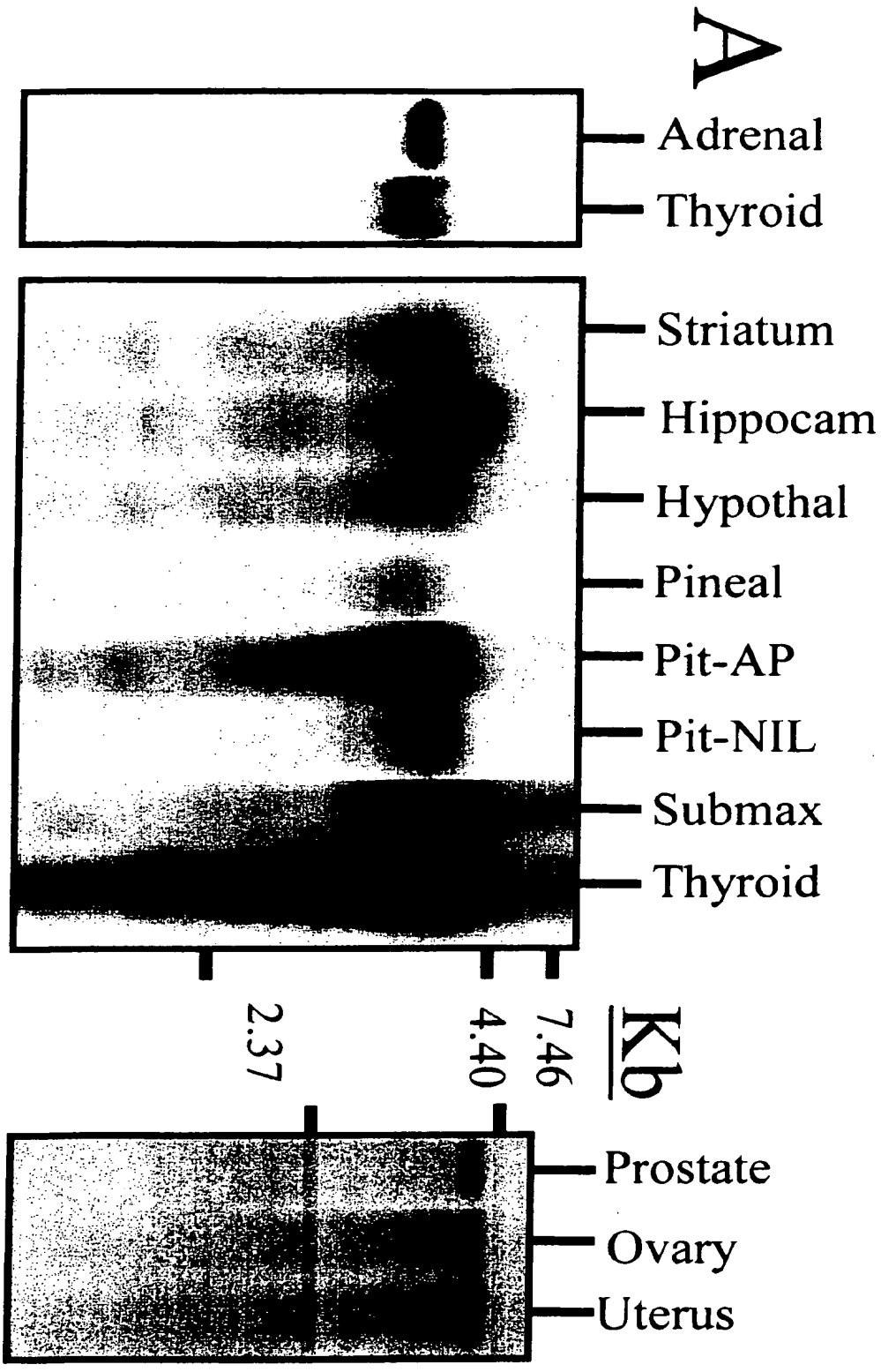
A
Adrenal
Thyroid
Striatum
Hippocam
Hypothal
Pineal
Pit-AP
Pit-NIL
Submax
Thyroid
2.37
4.40
7.46
Kb
Prostate
Ovary
Uterus

FIGURE 2A

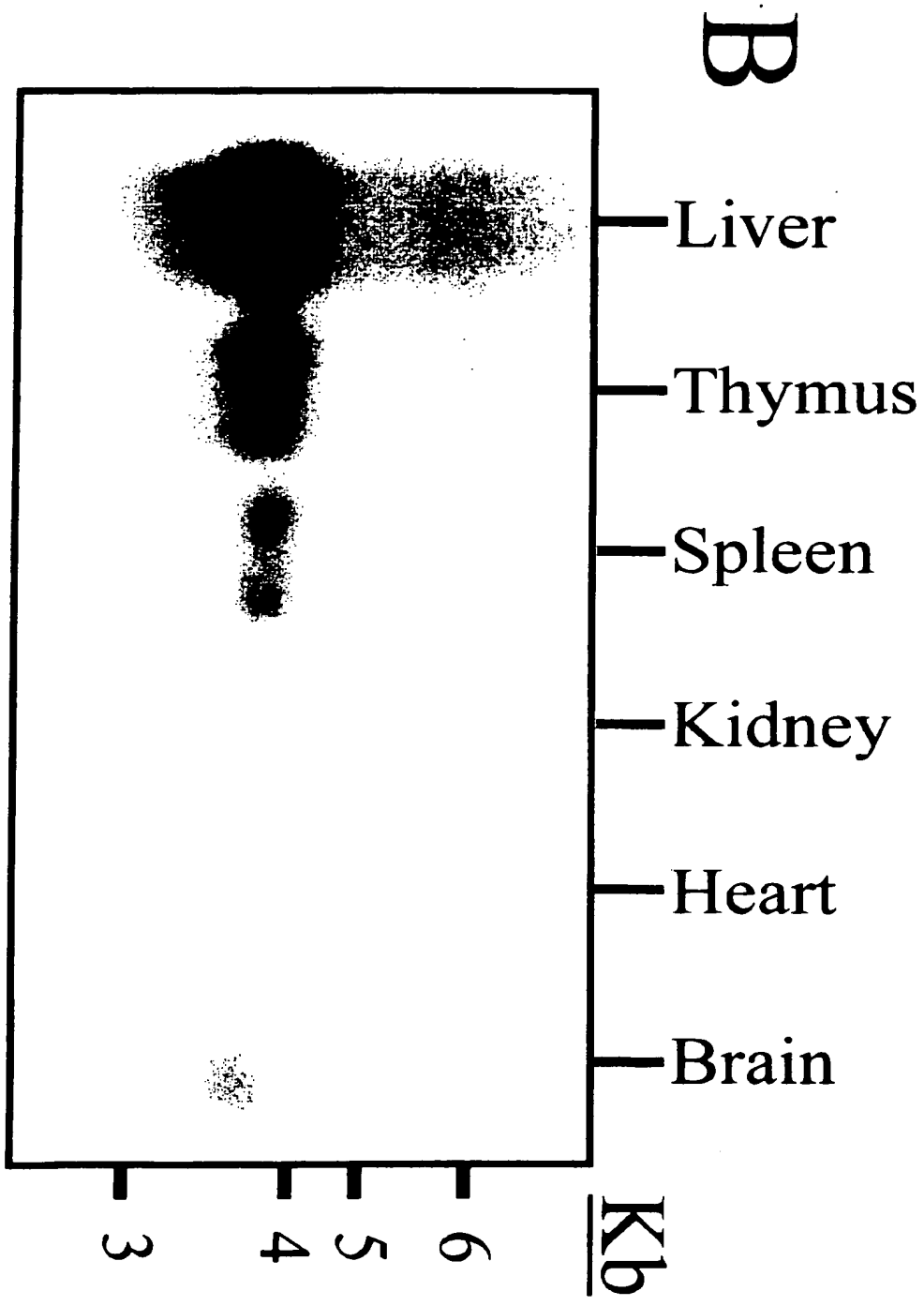

FIGURE 2B

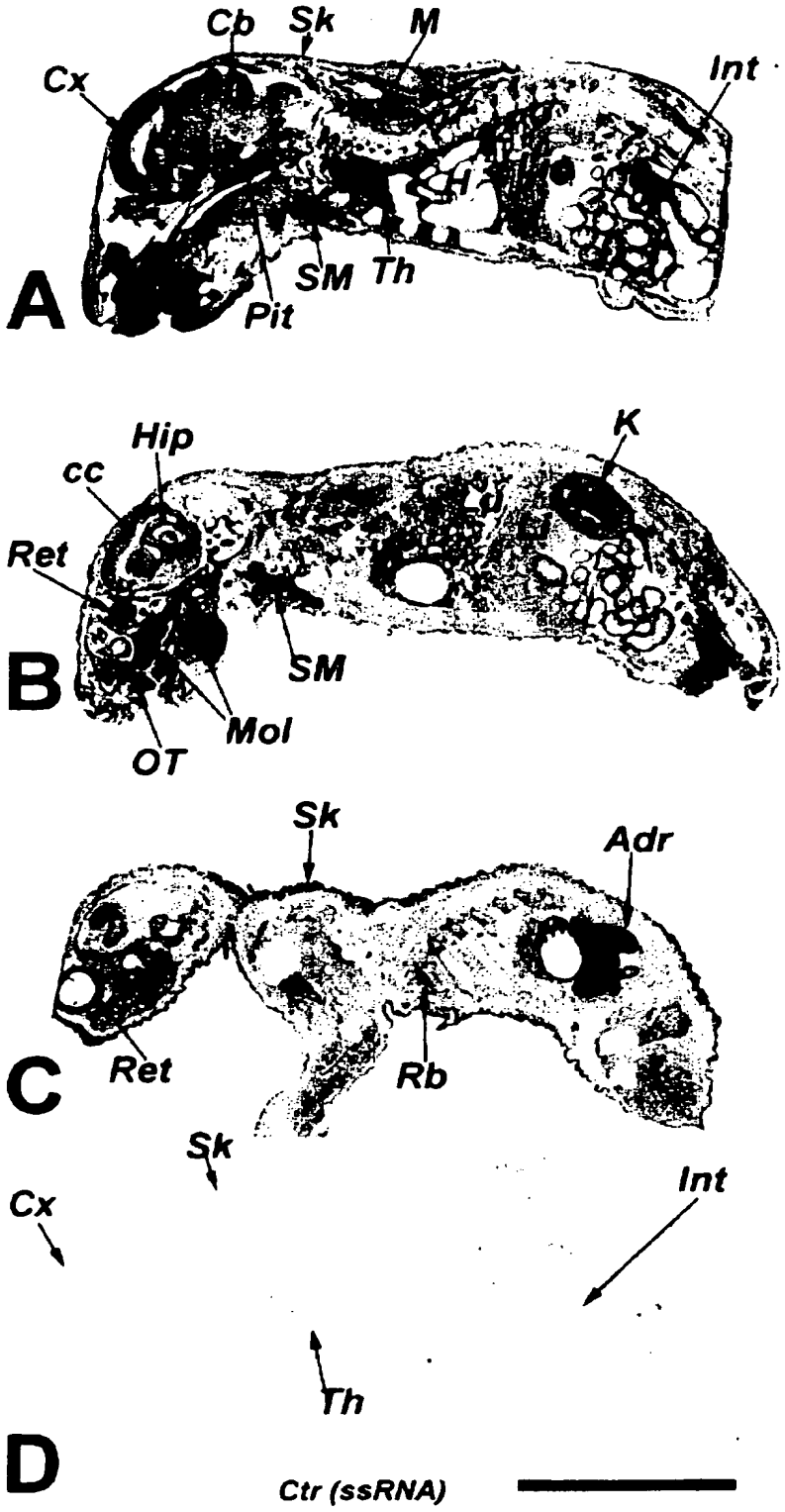
Cb
Sk
M
Cx
Int
H
SM
Th
A
Pit
Hip
K
cc
Ret
SM
B
Mol
OT
Sk
Adr
Ret
Rb
C
Sk
Int
Cx
Th
D
Ctr (ssRNA)

FGIURE 3

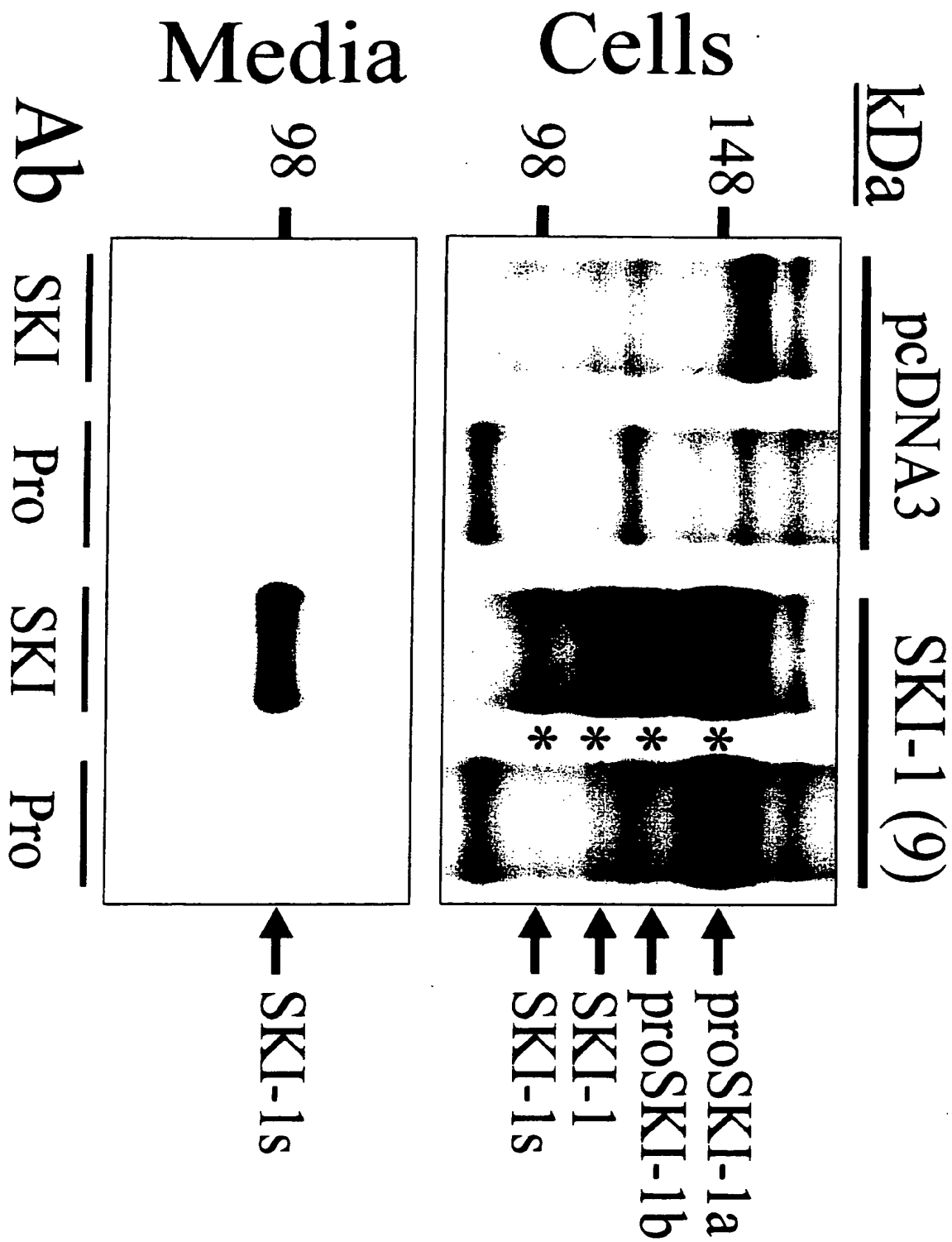
Media
Cells
kDa
98
98
148
Ab
SKI
Pro
SKI
Pro
pcDNA3
SKI-1 (9)
SKI-1s
SKI-1s
SKI-1
proSKI-1b
proSKI-1a

FIGURE 4

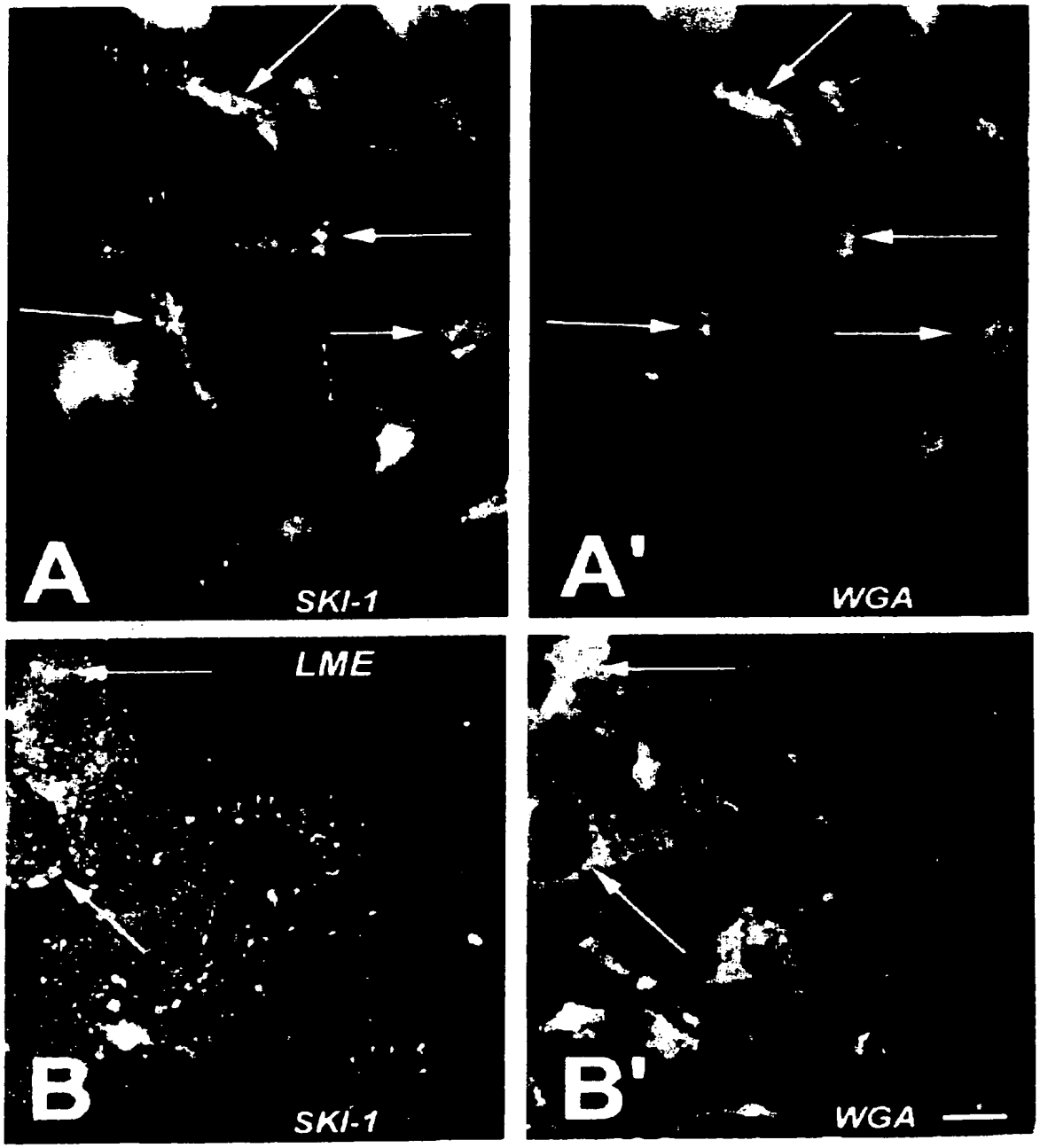

FIGURE 5

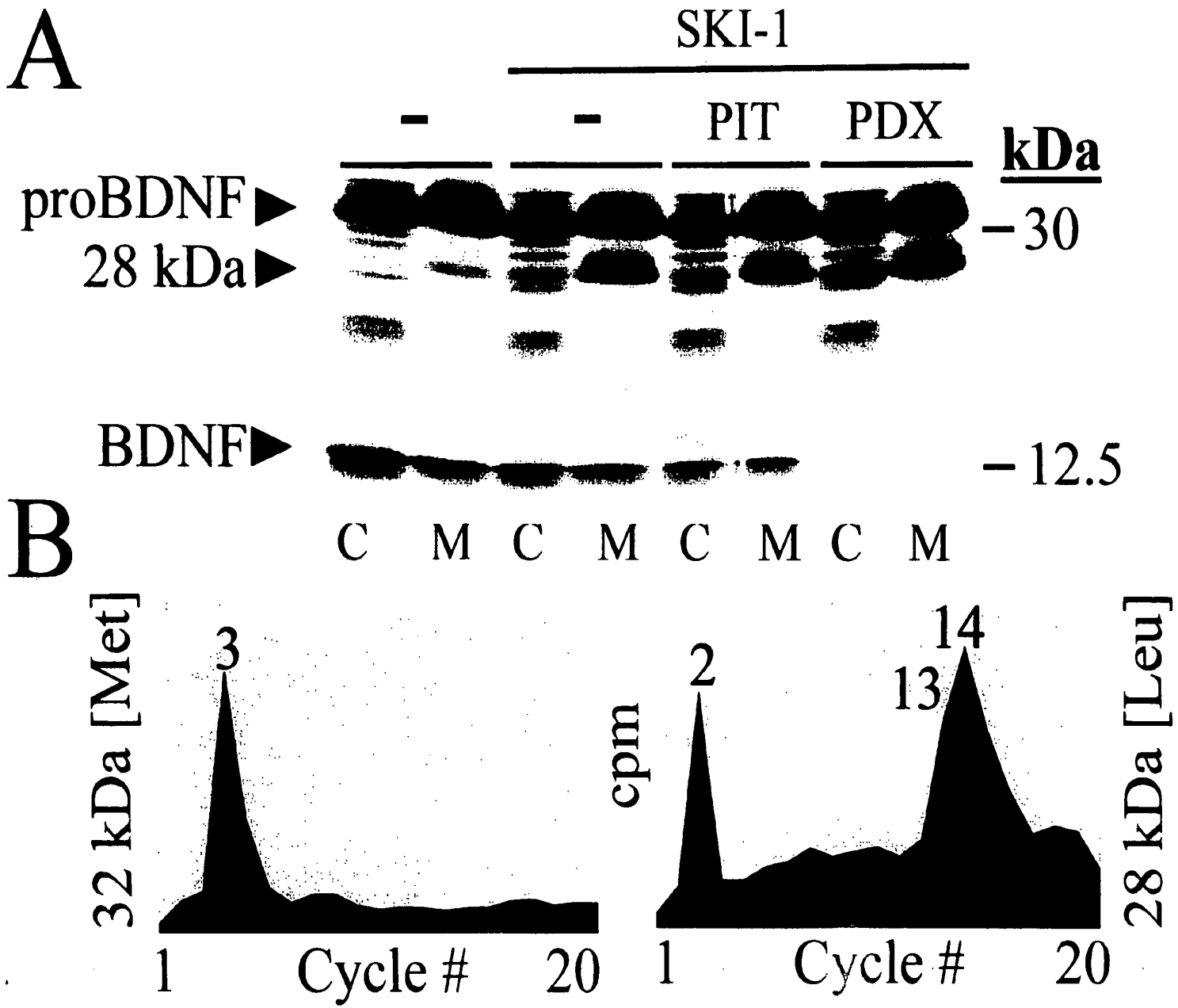

FIGURE 6

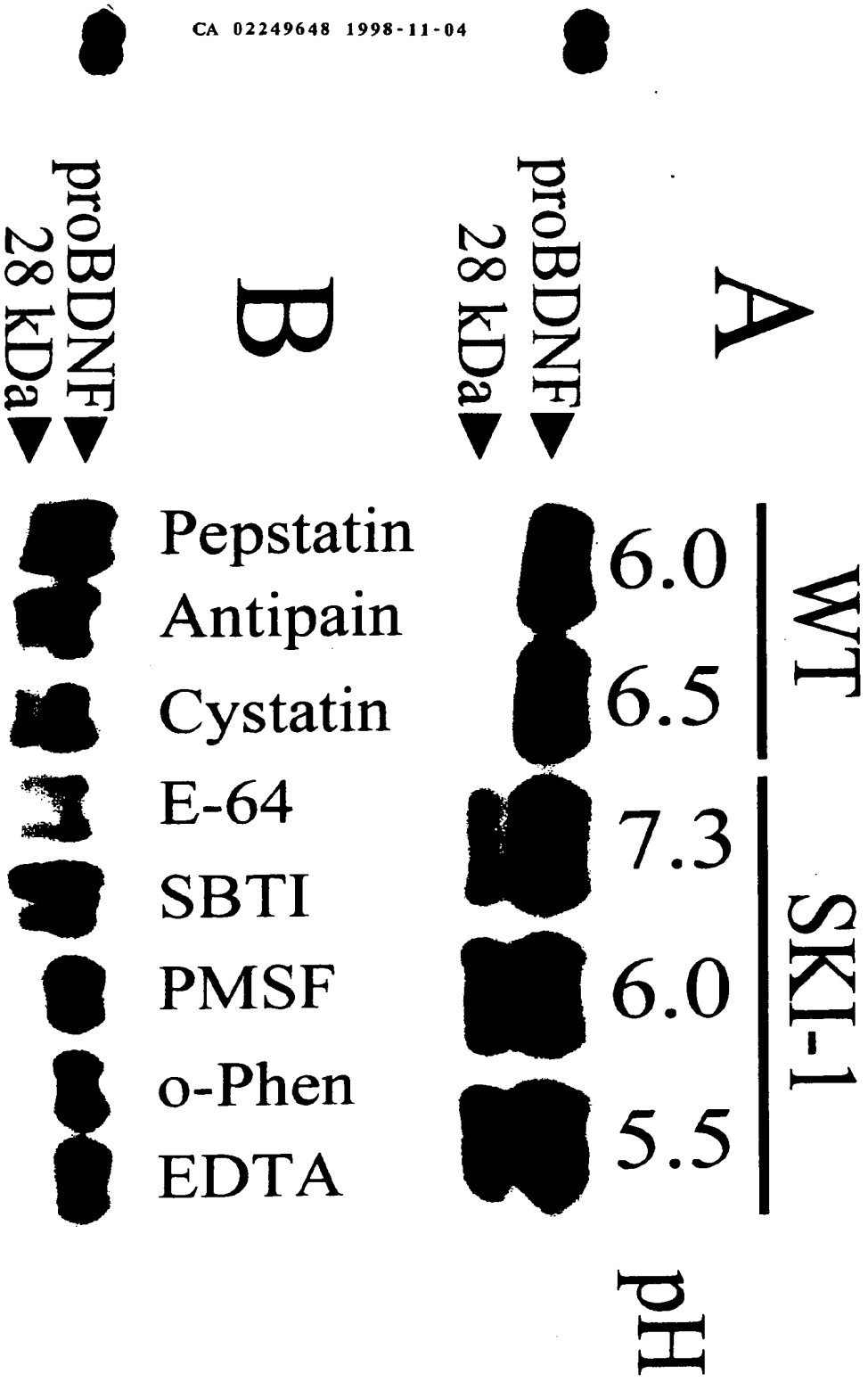
A
proBDNF
28 kDa
6.0
6.5
7.3
6.0
5.5
WT
SKI-1
pH
B
proBDNF
28 kDa
Pepstatin
Antipain
Cystatin
E-64
SBTI
PMSF
o-Phen
EDTA

FIGURE 7

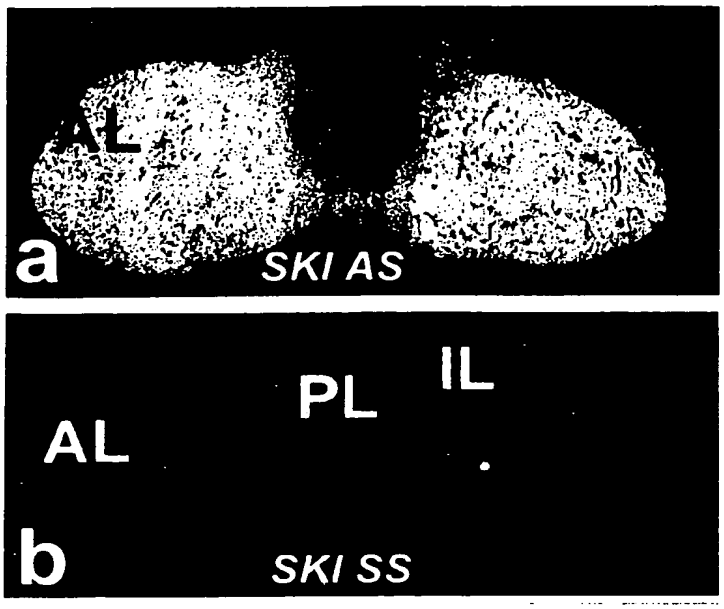

FIGURE 8

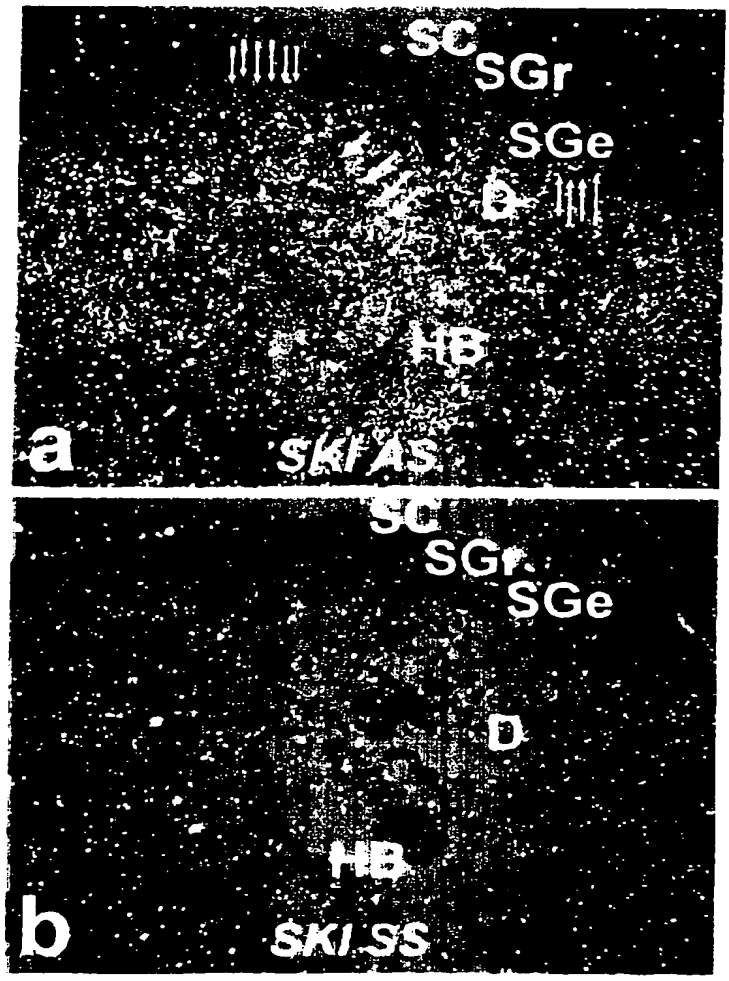

FIGURE 9

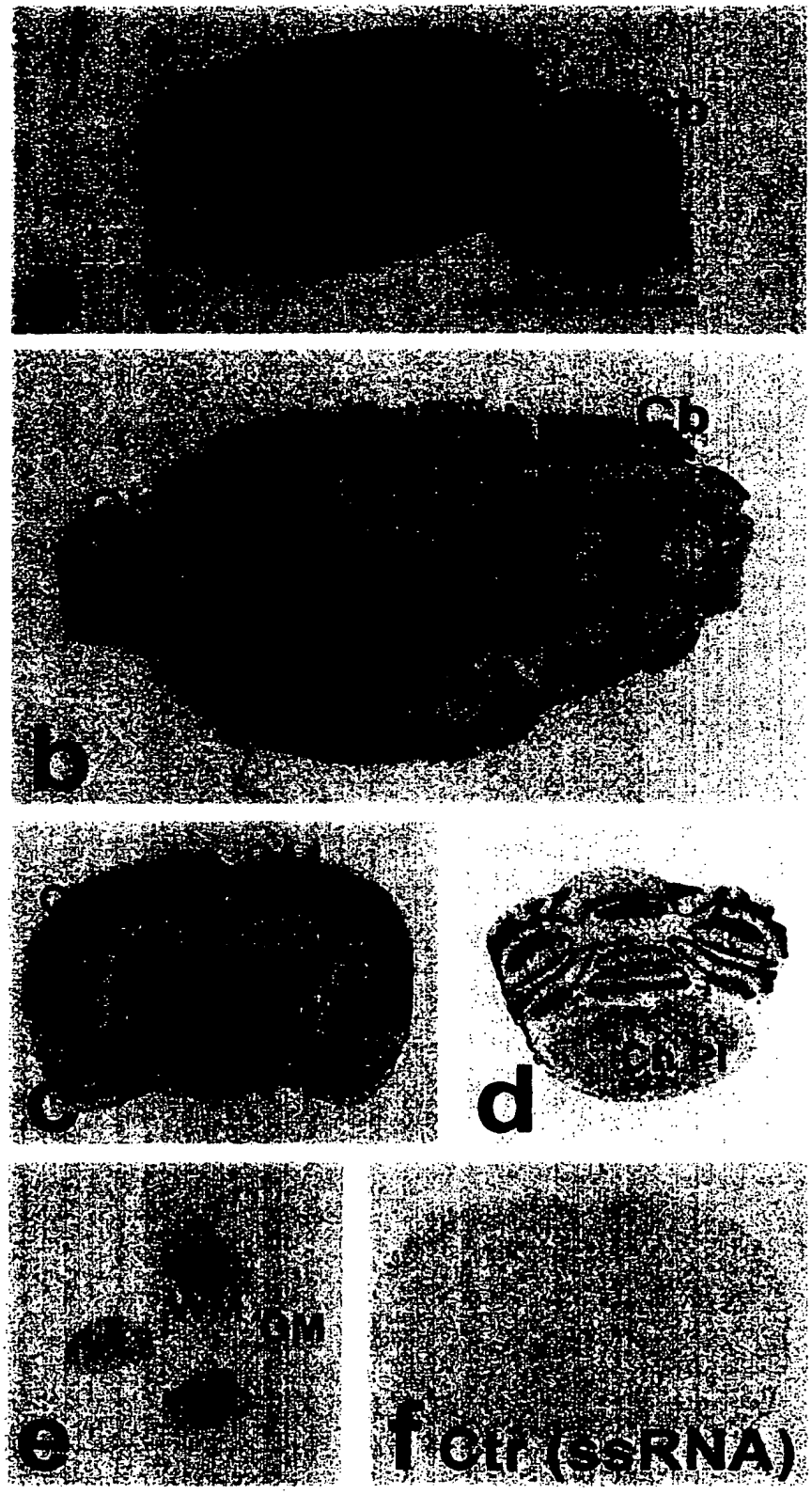

FIGURE 10

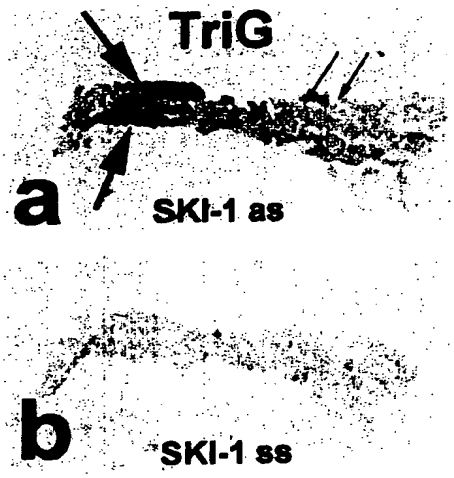

FIGURE 11

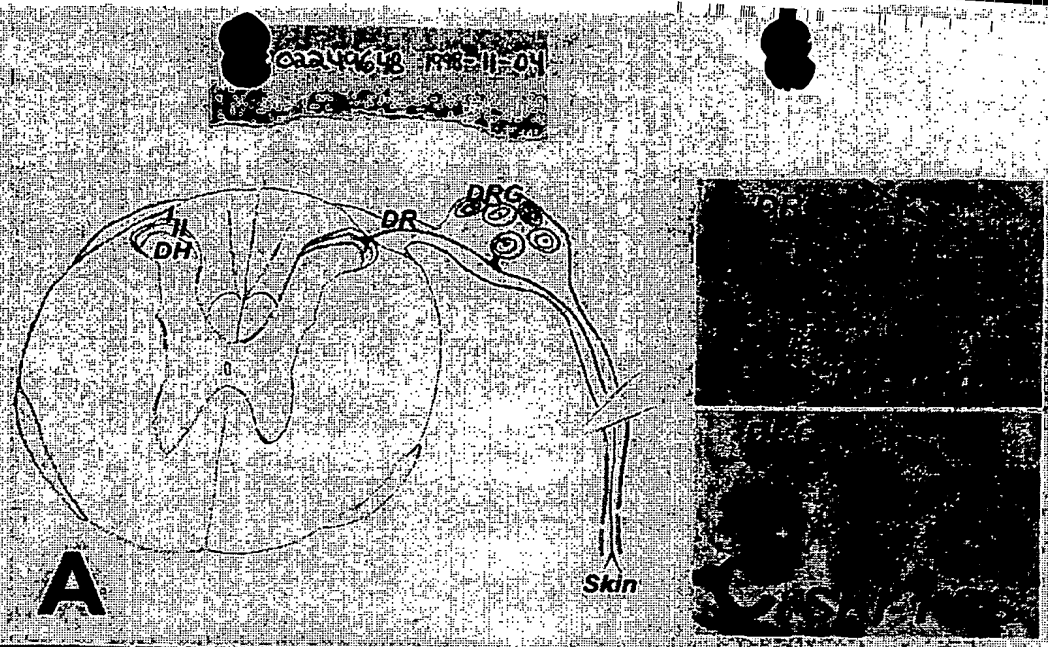

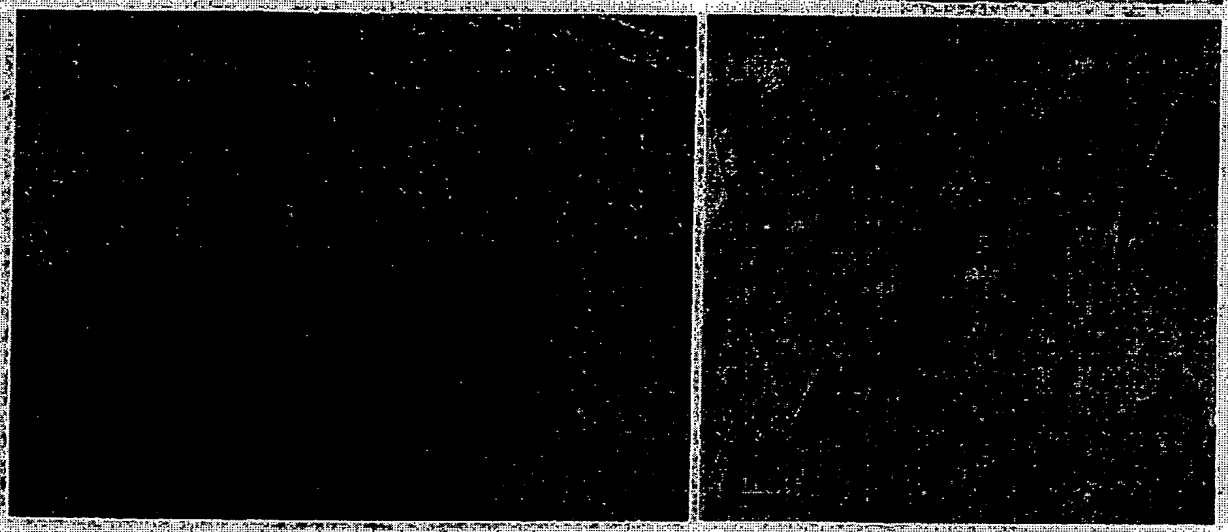

DRG Cx Cb Hip SpC Thyr Adr Stom

FIGURE 12